ARMY RESEARCH LABORATORY

Time-dependent Modeling of Brillouin Scattering in Passive Optical Fibers Pumped by a Chirped Diode Laser

by Jeffrey O. White, Steven D. Rogers, and Carl E. Mungan

ARL-TR-6113 **August 2012**

NOTICES

Disclaimers

The findings in this report are not to be construed as an official Department of the Army position unless so designated by other authorized documents.

Citation of manufacturer's or trade names does not constitute an official endorsement or approval of the use thereof.

Destroy this report when it is no longer needed. Do not return it to the originator.

Army Research Laboratory
Adelphi, MD 20783-1197

ARL-TR-6113 **August 2012**

Time-dependent Modeling of Brillouin Scattering in Passive Optical Fibers Pumped by a Chirped Diode Laser

Jeffrey O. White, Steven D. Rogers, and Carl E. Mungan
Sensors and Electron Devices Directorate, ARL

REPORT DOCUMENTATION PAGE

Form Approved
OMB No. 0704-0188

1. REPORT DATE *(DD-MM-YYYY)*	2. REPORT TYPE	3. DATES COVERED (From - To)
August 2012	Final	June 2010 to June 2012

4. TITLE AND SUBTITLE
Time-dependent Modeling of Brillouin Scattering in Passive Optical Fibers Pumped by a Chirped Diode Laser

5a. CONTRACT NUMBER

5b. GRANT NUMBER

5c. PROGRAM ELEMENT NUMBER

6. AUTHOR(S)
Jeffrey O. White, Steven D. Rogers, and Carl E. Mungan

5d. PROJECT NUMBER

5e. TASK NUMBER

5f. WORK UNIT NUMBER

7. PERFORMING ORGANIZATION NAME(S) AND ADDRESS(ES)
U.S. Army Research Laboratory
ATTN: RDRL-SEE-M
2800 Powder Mill Road
Adelphi, MD 20783-1197

8. PERFORMING ORGANIZATION REPORT NUMBER
ARL-TR-6113

9. SPONSORING/MONITORING AGENCY NAME(S) AND ADDRESS(ES)

10. SPONSOR/MONITOR'S ACRONYM(S)

11. SPONSOR/MONITOR'S REPORT NUMBER(S)

12. DISTRIBUTION/AVAILABILITY STATEMENT
Approved for public release; distribution unlimited.

13. SUPPLEMENTARY NOTES

14. ABSTRACT
The coupled partial differential equations describing stimulated Brillouin scattering (SBS) in a fiber are solved numerically. The SBS builds up from random thermal phonons when a laser beam of sufficient power is incident upon the fiber. We show that the SBS can be suppressed by linearly ramping the laser frequency at a rate of up to 10^{16} Hz/s. High chirp rates lead to an increased Brillouin spectral bandwidth and decreased gain. The resulting SBS suppression agrees well with an adiabatic model and with experimental results.

15. SUBJECT TERMS
stimulated Brillouin scattering, high power fiber lasers

16. SECURITY CLASSIFICATION OF:			17. LIMITATION OF ABSTRACT	18. NUMBER OF PAGES	19a. NAME OF RESPONSIBLE PERSON
a. REPORT	b. ABSTRACT	c. THIS PAGE	UU	18	Jeffrey O. White
Unclassified	Unclassified	Unclassified			19b. TELEPHONE NUMBER (*Include area code*) (301) 394-0069

Standard Form 298 (Rev. 8/98)
Prescribed by ANSI Std. Z39.18

Contents

List of Figures

Acknowledgments

We thank Curtis Menyuk and Brian Jenkins for useful discussions, and Steven Wandzura, Asaf David, and Moshe Horowitz for providing us with their computer codes that we used to help guide the writing of our own code. We also acknowledge financial support from the High Energy Laser Joint Technology Office contract 11-SA-0405.

INTENTIONALLY LEFT BLANK.

1. Introduction

Brillouin scattering is one of the lowest order nonlinear effects that arises in optical fibers and it, thus, limits the transmitted laser power P_L. Above a threshold laser power, P_{th}, the Brillouin scattering becomes stimulated rather than spontaneous, and the Stokes backscattered power P_S rises dramatically. Various methods have been devised to increase the threshold. In the present report, we analyze the effect of linearly sweeping the center frequency of the pump laser (while keeping its linewidth narrow) at a fast chirp rate β (in Hz/s). To be effective, the chirp must be large enough that the pump laser gets swept out of the Brillouin gain bandwidth $\Delta\nu_B$ within the transit time of the fiber, $t_f = nL/c$, where L is the length of the fiber, n is the core refractive index, and c is the speed of light. That is, one requires β to be large enough that $t_f >> t_c$, where $t_c = \Delta\nu_B/2\beta$. Here we analyze values of β up to 10^{16} Hz/s, corresponding to the upper range of chirping that has been demonstrated to date for a diode laser by ramping its current.

Section 2 explains how Brillouin scattering is simulated numerically in a fiber pumped by a chirped laser. Section 3 then presents the simulation results for a 6-km fiber. Such long fibers have a low threshold because $P_{th} \approx 21A/g_0L$ in the unchirped case, where A is the modal area and g_0 is the peak Brillouin gain coefficient. Consequently, low laser powers can be used to experimentally verify the simulations. Good agreement is found between theory and experiment. Next, section 4 presents results of the time-dependent simulations for a short fiber (L = 17.5 m) having characteristics similar to those used for high-power laser delivery. Correspondingly larger chirps are needed to suppress stimulated Brillouin scattering (SBS) in this case. The results are in good agreement with a simpler adiabatic model for the range of chirps explored.

2. Theory for the Dynamic Simulations

The Brillouin scattering is modeled by three complex coupled partial differential equations (PDEs):

$$\frac{\partial E_L}{\partial z} + \frac{n}{c}\frac{\partial E_L}{\partial t} = -\frac{\alpha}{2}E_L + i\kappa E_S\rho\,, \tag{1a}$$

$$\frac{\partial E_S}{\partial z} - \frac{n}{c}\frac{\partial E_S}{\partial t} = \frac{\alpha}{2}E_S - i\kappa E_L\rho^*, \text{ and} \tag{1b}$$

$$\frac{\partial \rho}{\partial t} + \pi\Delta\nu_B\rho = i\Lambda E_L E_S^* + f\,. \tag{1c}$$

Here, the laser electric field $E_L(z,t)$, Brillouin Stokes-shifted electric field $E_S(z,t)$, and density variation $\rho(z,t)$ of the fiber from its mean value ρ_0 depend on time t and longitudinal position z (varying from $z = 0$ at the front face of the fiber to $z = L$ at the rear face). The spectral full-width-at-half-maximum (FWHM) of the spontaneous Brillouin peak is $\Delta\nu_B$. For a silica fiber at an incident laser wavelength of $\lambda_L = 1.55$ μm, the index is $n = 1.447$, the mean density is $\rho_0 = 2210$ kg/m^3, and the speed of sound is $\upsilon = 5960$ m/s (*1*). The loss coefficient in the fiber is taken to be $\alpha = 0.2$ dB/km = 0.0461/km. The optic coupling parameter is

$$\kappa = \frac{\pi\gamma}{2n\rho_0\lambda_L M}, \tag{2}$$

where the electrostriction coefficient for a silica optical fiber is $\gamma = 0.902$ (*2*) and the polarization is presumed to be completely scrambled in the fiber so that $M = 1.5$ (*3*). The acoustic coupling parameter is

$$\Lambda = \frac{\pi n\varepsilon_0\gamma}{\lambda_L\upsilon}, \tag{3}$$

where ε_0 is the permittivity of free space. The Langevin noise source $f(z,t)$ is delta-correlated in time and space such that (*4*)

$$\langle f(z,t) f^*(z',t')\rangle = Q\delta(z-z')\delta(t-t'), \tag{4}$$

where the thermal phonons are described by the strength parameter

$$Q = \frac{4\pi kT\rho_0\Delta\nu_B}{\upsilon^2 A}. \tag{5}$$

Here, k is Boltzmann's constant, $T = 293$ K is room temperature, and A is the fiber modal area.

The three PDEs in equation 1 are solved by iterated finite-difference approximations on a grid of time and space points (*5*). The spatial step size dz is chosen to be small enough that a factor-of-two reduction does not change the final values in equation 7 by more than 10%. The temporal step size is $dt = n\,dz/c$. The boundary conditions are $E_S(L,t) = 0$ and

$$E_L(0,t) = \sqrt{\frac{2P_0}{nc\varepsilon_0 A}}\exp\left[i\pi\beta\left(t+nL/c\right)^2\right], \tag{6}$$

where P_0 is the constant incident laser power at $z = 0$. The imaginary part of the argument of the exponential gives the chirped phase, equal to the time integral of the change in the laser frequency at a rate of β in Hz/s, relative to the frequency at the rear face of the fiber at $t = 0$. The three complex fields are first calculated across the fiber up to $t = 20t_f$ to ensure that the initial relaxation oscillations (*6*) have decayed away. The equations are then iterated over five more transit times to acquire a statistical average. The transmitted laser power P_L and reflected Stokes power P_S are computed by averaging over those additional steps,

$$P_L = \tfrac{1}{2} nc\varepsilon_0 A\langle |E_L(L,t)|^2 \rangle \text{ and } P_S = \tfrac{1}{2} nc\varepsilon_0 A\langle |E_S(0,t)|^2 \rangle. \quad (7)$$

The results were checked by verifying that $P_L \approx (P_0 - P_S)\exp(-\alpha L)$, and agreement was found to within about 1% for zero chirp.

3. Dynamic Results for a Long Fiber Compared to Experiment

Here we calculate P_S as a function of P_0 for a 6-km single-mode fiber. The FWHM of the spontaneous Brillouin peak was measured to be $\Delta\nu_B$ = 39 MHz using an optical spectrum analyzer (OSA). Also, the fiber's modal area was measured by scanning a razor blade across the beam in the far field of the exit face. The mode field radius was then calculated to be r = 4.55 μm at the exit face.

The reflectivity P_S/P_0 is plotted in figure 1 for both an unchirped and a chirped laser. It approaches 100% for large incident powers, illustrating that Brillouin scattering limits the transmission through the fiber. The threshold (defined as the incident power at which the reflectivity is equal to 1%) is approximately two orders of magnitude larger in the chirped case than in the unchirped case. For incident powers well below threshold, the reflectivity levels off to a spontaneous value that is independent of chirp and is in good agreement with the experimentally measured value of $R_0 = (3.0 \pm 0.5) \times 10^{-6}$, with no free parameters.

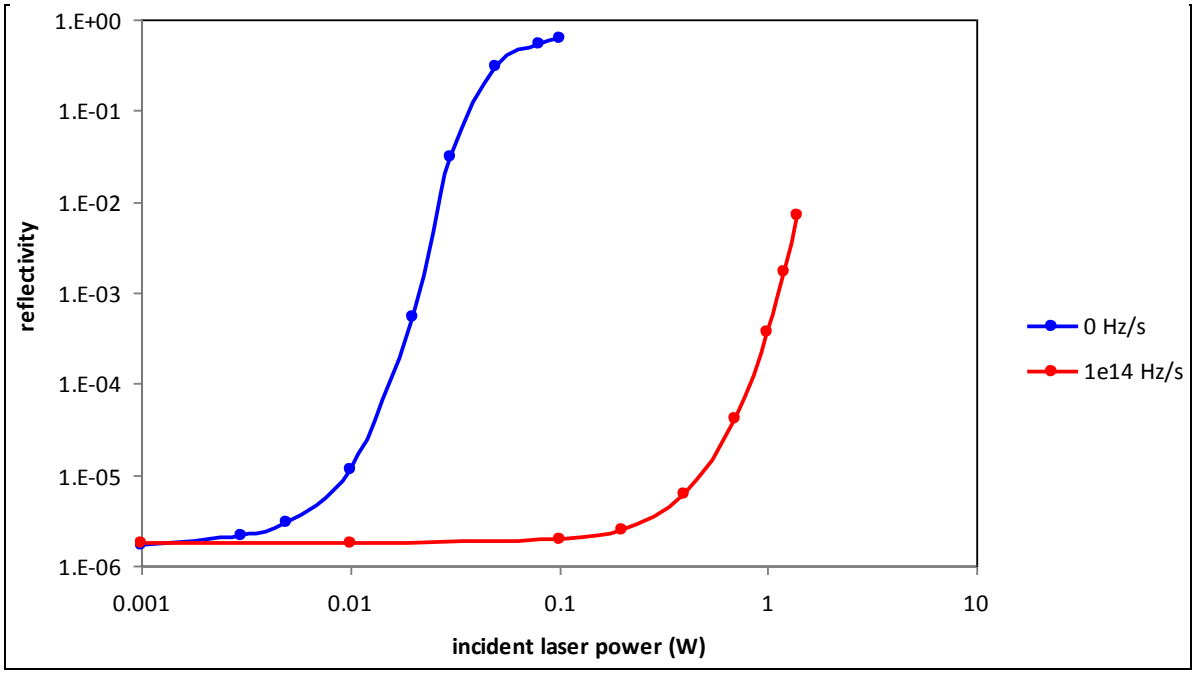

Figure 1. Brillouin reflectivity versus incident power for both an unchirped ($\beta = 0$) and a chirped (at $\beta = 10^{14}$ Hz/s) laser pumping a long fiber.

To directly compare these results to the experimental data, the total backscattered power is next plotted in figure 2 as a function of P_0. This backscattered power is the sum of the Brillouin Stokes power P_S and the Rayleigh power $P_R = 2.3 \times 10^{-4}\, P_0$. The Rayleigh backscattered power was determined from low-power measurements with an optical spectrum analyzer. There is reasonable agreement between theory and experiment.

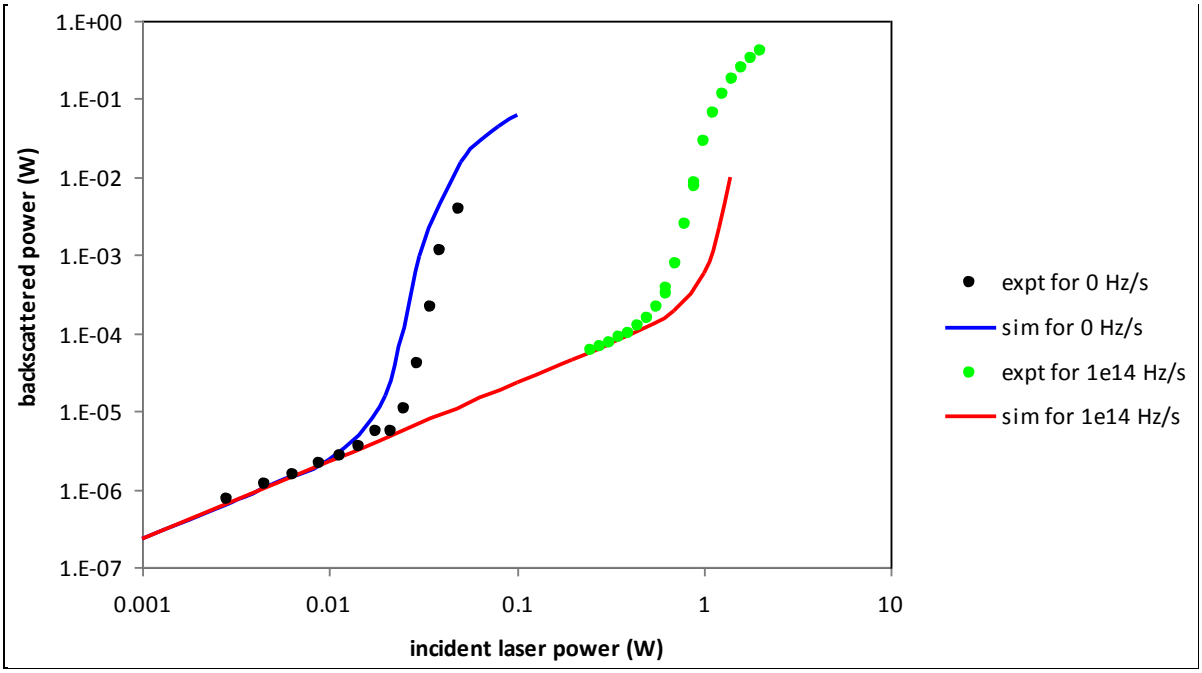

Figure 2. Comparison of the simulated and experimental (*7*) total backscattered power for the unchirped and chirped laser sources.

The peak value of the Brillouin gain coefficient is

$$g_0 = \frac{2\pi\gamma^2}{nc\rho_0 \upsilon \lambda_L^2 \Delta\nu_B M}, \tag{8}$$

which equals 6.4×10^{-12} m/W for the parameters given above. This value is a factor of 2 smaller than what is typically measured for fibers (*8*), possibly because of inhomogeneous broadening of the spontaneous Brillouin peak. According to equation 8, it is only the *product* $g_0\Delta\nu_B$ that should be the same for all polarization-scrambling silica fibers pumped at 1.55 μm and not their *individual* two values.

The power spectral density (in dBm/Hz) of the reflected Stokes electric field E_S (0,*t*) was computed as a function of frequency for each simulation run, and plotted up to the Nyquist limiting frequency. Lineshape functions were then fit to these spectra. The resulting FWHM are plotted as the blue dots in figure 3 for the long fiber at an incident laser power P_0 of 1 mW, well below threshold, for four different chirps. At the two lower chirps β of 10^{10} and 10^{12} Hz/s, the lineshapes were found to be Lorentzian, whereas at the two higher chirps of 5×10^{12} and

10^{13} Hz/s the lineshapes were Gaussian. The continuous red curve is a plot of the broadening expected in a simple model, namely

$$\Delta\nu = \Delta\nu_{\mathrm{B}} + nL\beta / c, \tag{9}$$

which fits the simulation results to within the error bars on the fitted widths.

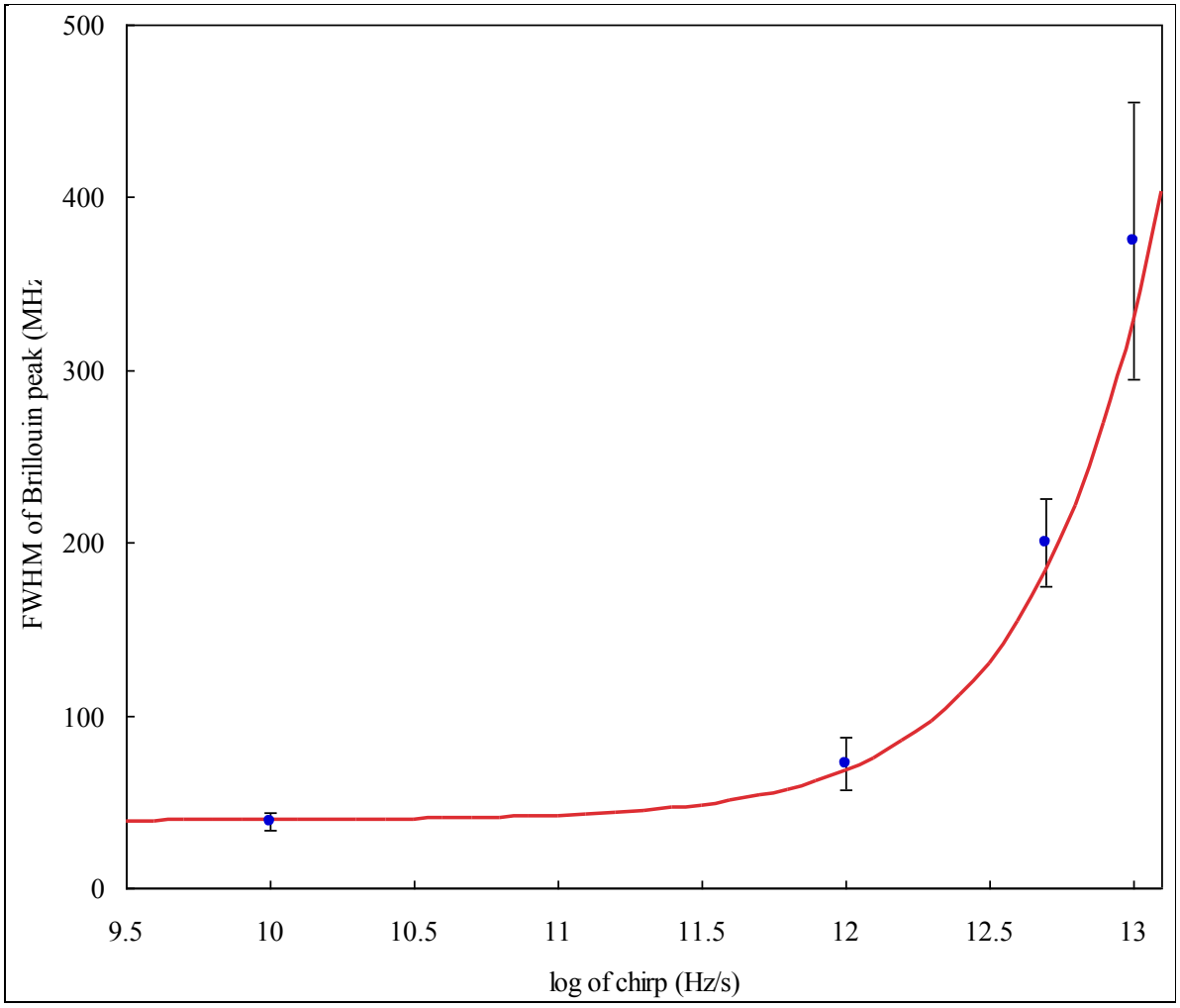

Figure 3. FWHM $\Delta\nu$ of the Brillouin peak as a function of the chirp β on a semilog scale.

4. Dynamic Results for a Short Fiber Compared to Other Models

Consider a shorter fiber having a length of L = 17.5 m, core radius of r = 13.75 μm, and spontaneous Brillouin FWHM of $\Delta\nu_{\mathrm{B}}$ = 20 MHz (corresponding to a peak Brillouin gain of g_0 = 1.2×10^{-11} m/W), as might be used to passively deliver a high-power laser beam. All other

parameters are taken to be the same as those listed in sections 2 and 3. The reflectivity is plotted in figure 4 for seven different values of the chirp β in Hz/s.

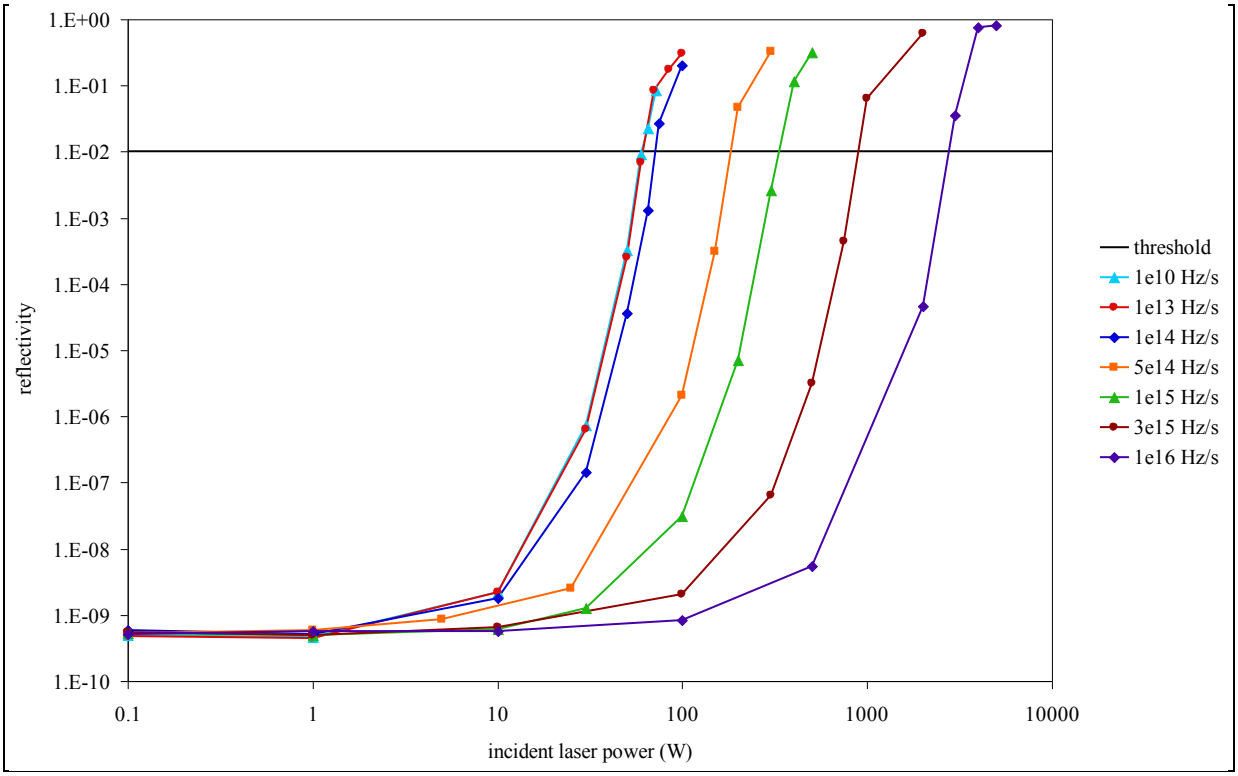

Figure 4. Brillouin reflectivity for a laser beam having a linear chirp β ranging between 10^{10} and 10^{16} Hz/s that is incident on a short fiber.

Well below threshold, the reflectivity has a constant value of $R_0 \approx 5 \times 10^{-10}$ independent of chirp and pump power. Jenkins' heuristic steady-state model (*1*) for the buildup of the spontaneous Stokes wave from thermal noise predicts that it should scale linearly with the effective absorption length of the fiber, $L_\alpha \equiv [1-\exp(-\alpha L)]/\alpha$, and be independent of $\Delta\nu_B$,

$$R_0 = \frac{2\pi^2 kT\gamma^2 L_\alpha}{Mn^2\rho_0 v^2 \lambda_L^2 A}. \qquad (10)$$

This equation implies $R_0 \approx 3 \times 10^{-9}$, which is only a factor of 6 larger than our simulation value. Similar agreement is found for the long fiber in section 3—equation 10 predicts $R_0 \approx 9 \times 10^{-6}$, whereas figure 1 has a low-power reflectivity of $R_0 \approx 2 \times 10^{-6}$.

The curves in figure 4 cross the 1% reflectivity line at the threshold incident laser powers, P_{th}. Those crossing points are plotted in figure 5 as the blue dots. At the maximum chirp of 10^{16} Hz/s, the threshold has increased by a factor of 50 compared to an unchirped pump source.

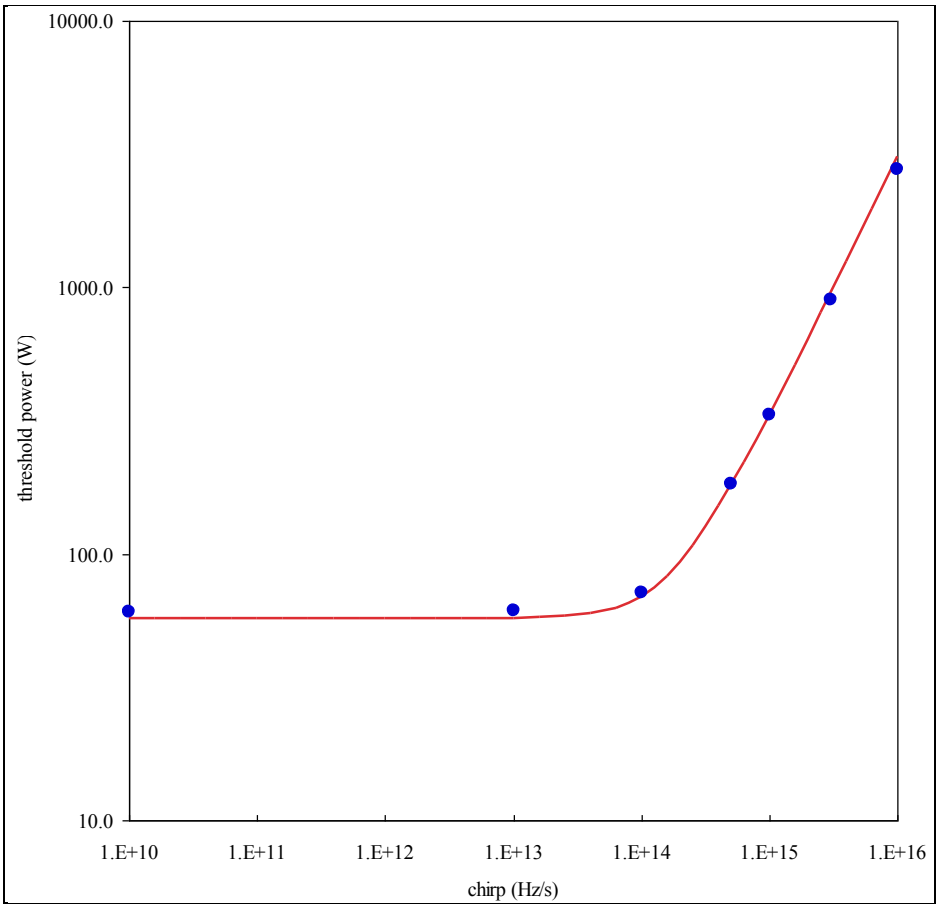

Figure 5. Threshold power P_{th} as a function of the chirp β on a semilog scale.

In figure 5, the threshold power scales linearly with the chirp β above 10^{14} Hz/s. One expects the threshold to increase as t_f/t_c, where the fiber transit time is $t_f = nL/c$ and the time required for the pump laser to chirp out of the Stokes bandwidth is $t_c = \Delta\nu_B/2\beta$. Combining a resonant integration of this adiabatic increase (*7*) with the familiar factor of 21 for the unchirped threshold value of g_0P_LL/A, one obtains

$$P_{th} = \frac{21A}{g_0 L}\frac{t_f / t_c}{\tan^{-1}(t_f / t_c)}. \tag{11}$$

Equation 13 is plotted as the red line in figure 5. The agreement with the time-dependent simulations is excellent, with no freely adjustable parameters. One can easily verify by graphing both sides that

$$\frac{t_f / t_c}{\tan^{-1}(t_f / t_c)} \approx 1 + \frac{t_f}{2t_c} \tag{12}$$

for values of t_f/t_c ranging from 0 to 6, thereby showing that equation 9 is consistent with the adiabatic model on which equation 11 is based.

5. Conclusion

Time-dependent numerical simulations show that SBS in optical fibers can be suppressed by linearly chirping the pump laser center frequency. One significant advantage of this method compared to competing techniques that broaden the pump laser with white noise is that a narrow linewidth is maintained at any given instant, enabling coherent combination of the outputs of several such fiber lasers to scale up to higher powers. Linear chirping enables a mismatch in the length of one such amplifier relative to another to be compensated by shifting the frequency at the input to that particular fiber using a modulator.

These dynamic simulations are in good agreement with experimental results for a 6-km fiber in the laboratory. The simulations should, therefore, also be valid for a short 17.5-m fiber having characteristics appropriate to high-power laser delivery systems. The time-dependent computer results for such a short fiber are in good agreement with a simpler adiabatic model, thereby validating use of that model to predict the performance of chirped fibers without requiring the demanding computer overhead of the full time-dependent calculations.

6. References

1. Jenkins, R. B.; Sova, R. M.; Joseph, R. I. Steady-state Noise Analysis of Spontaneous and Stimulated Brillouin Scattering in Optical Fibers. *J. Lightwave Tech.* **2007**, *25*, 763–770.
2. Melloni, A.; Frasca, M.; Garavaglia, A.; Tonini, A.; Martinelli, M. Direct Measurement of Electrostriction in Optical Fibers. *Opt. Lett.* **1998**, *23*, 691–693.
3. van Deventer, M. O.; Boot, A. J. Polarization Properties of Stimulated Brillouin Scattering in Single-mode Fibers. *J. Lightwave Tech.* **1994**, *12*, 585–590.
4. Boyd, R. W.; Rzazewski, K.; Narum, P. Noise Initiation of Stimulated Brillouin Scattering. *Phys. Rev. A* **1990**, *42*, 5514–5521.
5. David, A.; Horowitz, M. Low-frequency Transmitted Intensity Noise Induced by Stimulated Brillouin Scattering in Optical Fibers. *Opt. Express* **2011**, *19*, 11792–11803.
6. Bar-Joseph, I.; Friesem, A. A.; Lichtman, E.; Waarts, R. G. Steady and Relaxation Oscillations of Stimulated Brillouin Scattering in Single-mode Optical Fibers. *J. Opt. Soc. Am. B* **1985**, *2*, 1606–1611.
7. White, J. O.; Vasilyev, A.; Cahill, J. P.; Satyan, N.; Okusaga, O.; Rakuljic, G.; Mungan, C. E.; Yariv, A. Suppression of Stimulated Brillouin Scattering in Optical Fibers using a Linearly Chirped Diode Laser. *Opt. Express* (accepted **2012**).
8. Lanticq, V.; Jiang, S.; Gabet, R.; Jaouën, Y.; Taillade, F.; Moreau, G.; Agrawal, G. P. Self-referenced and Single-ended Method to Measure Brillouin Gain in Monomode Optical Fibers. *Opt. Lett.* **2009**, *34*, 1018–1020.

NO. OF COPIES	ORGANIZATION
1 ELEC	ADMNSTR DEFNS TECHL INFO CTR ATTN DTIC OCP 8725 JOHN J KINGMAN RD STE 0944 FT BELVOIR VA 22060-6218
1	US ARMY RSRCH DEV AND ENGRG CMND ARMAMENT RSRCH DEV & ENGRG CTR ARMAMENT ENGRG & TECHNLGY CTR ATTN AMSRD AAR AEF T J MATTS BLDG 305 ABERDEEN PROVING GROUND MD 21005-5001
1	US ARMY INFO SYS ENGRG CMND ATTN AMSEL IE TD A RIVERA FT HUACHUCA AZ 85613-5300
1	US GOVERNMENT PRINT OFF DEPOSITORY RECEIVING SECTION ATTN MAIL STOP IDAD J TATE 732 NORTH CAPITOL ST NW WASHINGTON DC 20402
6	US ARMY RSRCH LAB ATTN IMAL HRA MAIL & RECORDS MGMT ATTN RDRL CIO LL TECHL LIB ATTN RDRL CIO LT TECHL PUB ATTN RDRL SEE B C MUNGAN ATTN RDRL SEE O J WHITE ATTN RDRL SEE O S ROGERS ADELPHI MD 20783-1197